Simultaneous cleanup of Reactive Black 5 and cadmium by a desert soil bacterium

Ibtihel Louati[a,b], Jihene Elloumi-Mseddi[c], Wissem Cheikhrouhou[d], Bilel Hadrich[e], Moncef Nasri[a], Sami Aifa[c] and Tahar Mechichi[b*].

[a]Laboratory of Enzyme Engineering and Microbiology, National School of Engineers of Sfax, University of Sfax, BP 1173, 3038 Sfax, Tunisia.

[b]Laboratory of Biochemistry and Enzymatic Engineering of Lipases, National School of Engineers of Sfax, University of Sfax, 3038 Sfax, Tunisia.

[c]Laboratory of Molecular and Cell Screening Processes, Center of Biotechnology of Sfax, Sidi Mansour Road Km 6, BP 1177, 3018 Sfax, Tunisia

[d]LT2S laboratory, Digital Research Center of sfax, Technopark of sfax, BP 275, 3021 Sfax, Tunisia

[e] Unité de Biotechnologie des Algues, Biological Engineering Department, National School of Engineers of Sfax, University of Sfax, Tunisia.

* Correspondence to: Tahar Mechichi

E-mail: tahar.mechichi@enis.rnu.tn

Adress : ENIS route de soukra BP 1173, 3038 Sfax

Tel: 216 74 274 088

Fax: 216 74 275 595

Abstract

Multi-contaminated industrial wastewaters pose serious environmental risks due to high toxicity and non-biodegradability. The work reported here evaluated the ability of *Pseudomonas aeruginosa* strain Gb30 isolated from desert soil to simultaneously remove cadmium (Cd) and Reactive Black 5 (RB5), both common contaminants in various industrial effluents. The strain was able to grow normally and decolorize 50 mg L^{-1} RB5 within 24 h of incubation in the presence of 0.629 m mol L^{-1} of Cd^{2+}. In order to evaluate strain performance in RB5 detoxification, a cytotoxicity test using Human Embryonic Kidney cells (HEK293) was used. Cadmium removal from culture media was determined using atomic adsorption. Even in presence of (0.115 + 0.157 + 0.401 +0.381) m mol L^{-1}, respectively, of Cr^{6+}, Cd^{2+}, Cu^{2+} and Zn^{2+} in the growth medium, strain Gb30 successfully removed 35% of RB5 and 44%, 36%, 59% and 97%, respectively, of introduced Zn^{2+}, Cu^{2+}, Cr^{6+} and Cd^{2+}, simultaneously. In order to understand the mechanism of Cd removal used by *P. aeruginosa* strain Gb30, biosorption and bioaccumulation abilities were examined. The strain was preferentially biosorbing Cd on the cell surface, as opposed to intracellular bioaccumulation. Microscopic investigations using AFM, SEM and FTIR analysis of the bacterial biomass confirmed the presence of various structural features, which enabled the strain to interact with metal ions. The study suggests that *Pseudomonas aeruginosa* Gb30 is a potential candidate for bioremediation of textile effluents in the presence of complex dye-metal contamination.

Keywords: dyes; heavy metals; resistance; biodegradation; co-removal; biosorption.

1. Introduction

Progress in industrialization is a double-edged sword, improving the living conditions for humans, but at the same time negatively impacting the environment by discharging huge amounts of wastewater rich in organic and inorganic pollutants. Synthetic dyes and heavy metals, considered as hazardous xenobiotics, are major pollutants present in several industrial effluents (Huang et al., 2015; Ruta et al., 2010; Taştan et al., 2010). For example, Azo dyes, known to be the most widespread dyes used in several industrial processes, such as the manufacture of textiles, paints, pulp and paper, and in printing and tanning, generate highly toxic effluents (Aksu, 2005; Durai and Rajasimman, 2011; Mishra and Malik, 2014; Anwar et al., 2014; Sarker et al., 2015, Maqbool et al., 2016). As a result of these industrial processes, huge quantities of these compounds are discharged into the environment and cause serious ecological problems. Due to their chemical composition (aromatic rings, azoic linkages and amino groups), azo dyes are highly stable in both soil and aquatic environments (Imran et al., 2015). Several reports described the effects of these pollutants and their biodegradation products on living organisms (e.g. Mahmood et al., 2015). Other pollutants of great concern in industrial wastewaters are heavy metals. Cadmium is judged to be a major threat to both terrestrial and aquatic ecosystems and is present in a variety of industrial wastewaters (Pavlaki et al., 2016; Rani et al., 2014). It is considered an extremely hazardous metal due to both toxicity and carcinogenic properties, even at low doses (2.72 µg L^{-1}) (Bernhoft, 2013; Feki-Tounsi et al., 2013; Lacave et al., 2020; Pizzaia et al., 2019). Recent data suggested that human exposure to Cd induces multi-system toxicity. It can affect the cardiovascular, immune, urinary, nervous, endocrine and reproductive systems (Bernhoft, 2013). At the cellular level, Cd exposure induces expression of oxidative stress proteins, inhibition of DNA repair systems and induction of apoptosis (Rani et al., 2014). Previous reports confirmed the co-existence of Cd and dyes in textile and tannery effluents (Ali et al., 2009; Fenta, 2014; Sarker et al., 2015; Tchounwou et al., 2012). Despite wide experimental studies of biological remediation for the removal of dyes and heavy metals in recent years (Ali and El-Mohamedy, 2012; Aryal and Liakopoulou-Kyriakides, 2015; Ayangbenro and Babalola, 2017; Giovanella et al., 2017; Hansda et al., 2016; Solís et al., 2012), binary contamination with dyes and heavy metals remains a large environmental threat, but removal of these pollutants using biological has received little attention (Anwar et al., 2014; Huang et al., 2015; Maqbool et al., 2016; Taştan et al., 2010). Because industries require economically and environmentally sustainable wastewater treatments effective against a range of potential pollutants, examining the abilities of micro-organisms remove organic and inorganic xenobiotics from wastewaters is an urgent issue. Thus, the aim of the work reported here was to evaluate the potential of *Pseudomonas aeruginosa* strain Gb30 to simultaneously remove Reactive Black 5 and Cd in presence of a mixture of other heavy metals. The mechanisms through which strain Gb30 is able to tolerate heavy metal stress was also examined.

2. Materials and methods

2.1. Chemicals and reagents

Reactive Black 5 dye was purchased from Sigma-Aldrich (Germany). A stock solution with a final concentration of 10 g L^{-1} was prepared. The heavy metals stock solutions used were $CdCl_2$ (0.5 mol L^{-1}), $CuSO_4$ (0.25 mol L^{-1}), $K_2Cr_2O_7$ (1 mol L^{-1}) and $ZnSO_4$ (1 mol L^{-1}). Methanol used for HPLC was of analytical grade.

2.2. Bacterial strain, growth conditions and determination of the median effective concentration of RB5

Pseudomonas aeruginosa strain Gb 30 (KY655217.1) previously isolated from desert soil and characterized and identified in our laboratory, was selected for this work (Louati et al., 2019). Tolerance to Cd contamination was determined at the EC_{50} (10 hours) and represented the median effective concentration of Cd^{2+} able to cause 50% inhibition of bacterial growth after 10 hours incubation at 37°C. Examination of RB5 decolorization in the presence of Cd was carried out in LB medium, the pH of which was adjusted using standard NaOH and HCl solutions. Cultures were inoculated with 5% (v/v) from a pre-culture with an OD_{600nm} of 1.0 and supplemented with Cd^{2+} at a concentration corresponding to the EC_{50} (10 h). The initial pH was adjusted to 8 and 50 mg L^{-1} final concentration of dye added. Cultures were incubated at 37 °C, under static conditions. Aliquots for further analyses were withdrawn at 12 h intervals.

2.3. Effect of Cd^{2+} on bacterial growth and dye decolorization

Growth kinetics of control and Cd^{2+} containing cultures were evaluated by dry weight biomass determination during incubation. Color removal was analyzed using HPLC and UV-Visible spectroscopy. RB5 biodegradation products were examined by HPLC, using a DIONEX UltiMate 3000 (Thermo Scientific) C-18 column at room temperature. The mobile phase was water / methanol (60 / 40 %) with a flow rate of 1 mL min^{-1}. Compounds were detected using an UV/VIS detector at 597 nm.

Absorption of culture samples was scanned in the range of 200-800 nm using an UV-Visible spectrophotometer. Any RB5 remaining in the culture medium was determined by measuring the optical density of a sub-sample of the cultures in the range of 400-800 nm using a JENWAY 7315 UV/Vis spectrophotometer. To investigate the effect of Cd^{2+} ion concentration on RB5 removal, the decolorization rate was calculated for the first 24 h of incubation by plotting RB5 decolorization yield at different Cd^{2+} concentrations.

2.4. Cytotoxicity assessment of RB5 decolorization products

2.4.1. Cytotoxicity assessment

Changes in cytotoxicity was examined based on the inhibitory effect of RB5 biodegradation products on proliferation of the HEK293 (Human Embryonic Kidney cells 293) cell line. RB5 biodegradation products were obtained after incubation of *P. aeruginosa* Gb30 for 24 h under static condition at 37 °C in presence of 300 mg L^{-1} of dye. The culture medium was centrifuged at 6000 rpm for 20 min at 4 °C and the supernatant filtered through 0.45 µm filters before using directly in the cytotoxicity assays. Cultures without dye and with untreated RB5 (300 mg L^{-1}) were considered as negative and positive controls, respectively. HEK293 cells were cultured in 96-well plates, containing DMEM supplemented with 10% foetal bovine serum, 50 IU mL^{-1} penicillin, 50 mg mL^{-1} streptomycin, and incubated at 37 °C in a humidified 5% CO_2 atmosphere until 40% confluence. The appropriate concentrations of the prepared samples were added and cell cultures incubated for 48 hours. Culture run added with DMEM corresponds to negative response.

2.4.2. MTT assay

The MTT test, based on the reduction of 3-(4,5-dimethylthiazol-2-yl)-2,5-diphenyltetrazolium bromide (MTT) into purple formazan crystals by succinate dehydrogenase in the mitochondrial respiratory chain of the HEK293 cells, was used to assess viability. After incubation, the culture medium was removed and cells washed twice in PBS1X. Fresh medium (100 µL) containing 10 µL MTT solution (5 mg mL^{-1} in PBS) was added. Four hours later, in order to dissolve the formazan, 100 µL of 10% SDS solution was added to each well. Optical density was measured at 570 nm using a Varioskan microplate reader (Thermofisher). Percentage cell survival in the presence of untreated and degraded RB5 was calculated as follows:

$$cell\ survival\ (\%) = \frac{A_T}{A_C} * 100 \qquad Eq\ (1)$$

Where:

A_T: is the absorbance at 570 nm of treated cells

$A_{C:}$ is the absorbance at 570 nm of control cells

2.5. Heavy metal removal

2.5.1. Metal removal kinetics

Residual Cd^{2+} ion concentration in the culture medium was determined by atomic absorption (Fisher Scientific ice 3000) at 12 hour intervals. To investigate the adsorption process, pseudo-first and pseudo-second order kinetic models were fitted to the experimental data. The pseudo-first order model equation proposed by Lagergren (Lagergren, 1898) assumes that the rate of occupation of sorption sites is proportional to the number of unoccupied sites and is expressed as follows:

$$q = q_{eq} \cdot \left(1 - e^{-k_1 . t}\right) \qquad Eq\ (2)$$

Where

q: quantity of Cd biosorbed per unit of mass of cells

q_{eq}: quantity of Cd biosorbed per unit of mass of cells at equilibrium

k_1 (min $^{-1}$) is the adsorption rate constant.

The pseudo-second order model described by Ho and McKay (Ho and McKay, 1999) assumes that adsorption follows second order chemisorption. This model was used to explain the sorption kinetics using the following expression:

$$q = \frac{k_2 \cdot q_{eq}^2 \cdot t}{1 + k_2 \cdot q_{eq} \cdot t} \qquad Eq\ (3)$$

where k_2 (g mg^{-1} min) is the adsorption rate constant of the pseudo-second order adsorption.

Cd removal in the presence of a mixture of three heavy metals (Zn^{2+}, Cu^{2+} and Cr^{6+}), containing EC_{50} (10 h)/4 of each heavy metal concentration (equivalent to 0.115 + 0.157 + 0.401 +0.381 m mol L^{-1} of Cr^{6+}, Cd^{2+}, Cu^{2+} and Zn^{2+}, respectively, was also investigated. The ability of strain Gb30 to remove several heavy metals simultaneously was assessed by atomic adsorption analysis of residual heavy metals in the mixture.

2.5.2. Bioaccumulation and biosorption assays

In order to understand Cd uptake by *P. aeruginosa* strain Gb30, adsorption of the metal to the bacterial surface and accumulated inside the cell was determined. Briefly, LB culture medium containing EC_{50} (10h) $CdCl_2$ and 50 mg L^{-1} RB5 was inoculated with 5% from a culture of strain Gb30 (DO= 1.0) and incubated for 24 h at 37 ºC. After incubation, bacterial cells were harvested by centrifugation at 6000 rpm, 4°C, and washed 3 times in milliQ water with repeated centrifugation. Subsequently, the pellet was suspended in 10 mL of 20 Mmol L^{-1} ethylenediaminetetraacetic acid (EDTA) and left-over night for desorption of the cell surface bound Cd. After centrifugation, the quantities of Cd accumulated inside the cells and adsorbed on the cell surface were measured in the bacterial pellet and the supernatant by atomic absorption (Fisher Scientific ice 3000).

2.5.3. Morphological analysis

2.5.3.1. Fourier transform infrared spectroscopy (FTIR)

In order to investigate the potential functional groups responsible for Cd^{2+} ion uptake on *Pseudomonas aeruginosa*, bacterial biomass grown in the presence and in absence of Cd^{2+} was collected, washed twice in milliQ water, lyophilized and the IR spectrum recorded in the range 650-4000 cm^{-1} on a Cary 630 FTIR, Agilent technologies spectrophotometer.

2.5.3.2. Scanning Electron Microscopy (SEM)

The effect of heavy metals on bacterial cell morphology was examined using SEM. Bacterial pellets were prepared from cultures with and without Cd, as described above, fixed in 4 % formaldehyde in phosphate buffer for 30 min and washed three times in 0.1 mol L^{-1} phosphate buffer solution (pH 7.4). Samples were dehydrated in serial ethanol dilutions (25%, 50%, 60 %, 70%, 80%, 90% and 100%) before sputter coating (cathodic spraying) with gold. Cell morphology was evaluated using a JEOL (JFC-1100E) scanning electron microscope using an accelerating voltage of 15 kV.

2.5.3.3. Atomic Force Microscopy (AFM)

AFM analysis of cells grown in control cultures and in heavy metal-stressing conditions is a means of assessing toxicity. Damaged cell morphology can clearly illustrated using AFM through high resolution topographical images of cell surfaces. For AFM analysis samples were prepared according to Chao and Zhang (2011). Bacteria cultured in presence and absence of Cd^{2+} ions were harvested and washed twice in PBS, fixed in 4 % paraformaldehyde, washed in deionized water and placed on a previously prepared clean glass slide for air drying. Glass slides were left overnight in ethanol/HCl (70:1/v:v) before sonicating twice for 10 min in sterilized deionized water. The washed slides were dried at room temperature in sterile Petri dishes. AFM micrographs were recorded with silicon cantilever Tap190Al-G with force constant 48 N/m, in the distance mode via the Nanosurf Easyscan 2 Controller. The data generated from some of the AFM height images were used to calculate surface roughness of the bacterial cell exterior. The root mean square (R_{rms}), corresponding to the roughness of the samples, was calculated with the following expression:

$$R_{rms} = \sqrt{\sum_{i=1}^{N} \frac{(z_i - z_m)^2}{(N-1)}} \qquad Eq(4)$$

where, N is the total number of data points, z_i is the roughness of the i^{th} point,z_m is the average roughness.

2.6. Statistical analysis

Data were summarized as the mean±SD of three independent experiments. Comparisons between treatments for all experiments were performed using the Student's test, with significance at $P \leq 0.05$.

Kinetics models as well as parameter estimation for each model were fitted to non-linear regression models using Matlab R2010a (The Math Works, USA) software. The quality of fit for each model fitting was tested by calculating coefficient of determination (R^2), adjusted coefficient of determination (R^2_{adj}), root mean squared error (RMSE) and sum of squared error of prediction (SSE). The best model was chosen from the comparison between the four defined statistical criteria.

3. Results and discussion

3.1. Effect of Cd^{2+} ions on growth and RB5 decolorization

The effect of addition of Cd^{2+} on growth and decolorization ability of *P. aeuriginosa* Gb30 was examined. In the first ten hours of incubation, the EC_{50}(10h) of $CdCl_2$ was estimated to be 0.629 m mol L^{-1}. At this concentration, bacterial growth was slightly affected for the first 24 h, but proceeded normally for the next 48 h compared to Cd-free cultures. As decolorization was a rapid process, RB5 removal from the culture medium in presence of EC_{50}(10h) of $CdCl_2$ was affected in the first 12 h of incubation, but reached a maximum at 24 h (Fig.1). After 12 h incubation, 75% and 25% of the initial RB5 concentration was removed in the Cd-free and Cd-containing cultures, respectively; totally degradation had occurred by 24 h for both cultures. UV-Vis spectra of RB5 decolorization over 72 h confirmed that decolorization was total finished within the first 24 h of incubation (Fig.2). Compared to the untreated dye, HPLC spectra of RB5 biodegradation in the presence Cd^{2+} after 24 h of incubation confirmed the total degradation of the dye; new peaks that appeared in the spectra corresponded to the degradation products (Fig.2). Decolorization rate was slightly decreased in cultures as the Cd^{2+} ion concentrations reached 100 mg L^{-1}. The decolorization rate decreased from 2.25 to 1.7 mg L^{-1} h^{-1} between Cd concentrations from zero to 100 mg L^{-1}. Above this concentration, a sharp decrease in the decolorization rate occurred, and the process was totally inhibited at 250 mg L^{-1}.

Increasing concentrations of Cd^{2+} ions also extended the lag phase for decolorization (Soni et al., 2014). Although Cd is known to be toxic through disruption of the cellular enzymatic systems and oxidative damage to DNA (Gui et al., 2017), strain Gb30 exhibited high resistance toward Cd^{2+} ions and decolorization processed normally at high Cd concentrations. This result suggests the existence of an efficient enzymatic system able of degrading azo dyes co-existing in solution with Cd. Increasing heavy metal concentrations in culture media damages cell growth, probably based on competition by Cd^{2+} ions for metabolic sites in enzymes such as reductases, which require essential metals for activity. There are previous reports on the ability of *P. aeruginosa* strains to decolorize dyes in the presence of different heavy metals (Maqbool et al., 2016; Soni et al., 2014).

3.2. Cytotoxicity assessment of RB5 decolorization products

3.2.1. MTT test

Survival of HEK293 cells in cultures to which RB5 biodegradation products were added was significantly higher ($p \leq 0.05$) compared to cells cultured in the presence of 300 mg L^{-1} untreated dye (Fig.3). At a concentration of 300 mg L^{-1}, the azo dye clearly caused a cytotoxic response, decreasing cell viability by 50% with respect to the control treatment, while the biodegradation products were less toxic to HEK293. Although several previous studies suggested that decolorization does not always lead to detoxification (Ben Mansour et al., 2009; Dellai et al., 2013), the results obtained in the present work confirmed that *P. aeruginosa* Gb30 was able not only to decolorize but also to detoxify RB5. Similar findings were obtained by Kolekar and Kodam (2012) based on the MTT assay using the L-929 cell line to evaluate degradation products of Reactive Blue 59 by *Alishewanella* sp. KMK6.

3.3. Cd removal in multi-heavy metal containing medium

Examination of Cd removal in dye-containing medium over 72 h demonstrated that strain Gb30 removed more than 50% and 70% of the 0.629 m mol L^{-1} of added Cd, respectively, within 12 and 24 h. Cd uptake was constant for the remaining 48 h of incubation. These data showed that both pseudo-first and pseudo-second order models correlated well with the experimental findings (Table 1). However, the pseudo-first-order model was found to fit most closely (R2 ≥ 0.989), compared with the second model. These results suggest that the Lagergren kinetic model best described the adsorption of Cd onto bacterial biomass. The media containing multiple metals in mixture (0.115 + 0.157 + 0.401 + 0.381 m mol L^{-1} of Cr^{6+}, Cd^{2+}, Cu^{2+} and Zn^{2+}, respectively) showed that Cd was removed to a greater extent than the other heavy metals. Strain Gb30 not only removed the dye-Cd complex from the culture medium, but also removed other metal ions, reducing concentrations of Zn^{2+}, Cu^{2+}, Cr^{6+} and Cd^{2+} by 44, 36, 59 and 97%, respectively, at the same time (Fig.4). Cd removal was 97% in the first 12 h of culture, despite the presence of other heavy metals in the culture medium (Fig. 4). However, exposure to multiple metal ions clearly reduced RB5 degradation, as the decolorization yield was only 35% after 24 h of incubation (data not shown). The decrease in Cd uptake from 0.44 m mol L^{-1} in the single metal solution as compared to to 0.15 m mol L^{-1} in the multi-metal containing culture can be attributed to saturation of metal-binding sites responsible for heavy metal uptake on the cell surface (Giovanella et al., 2017). This study was unique in that *P. aeruginosa* Gb30 efficiently and simultaneously removed Cd and RB5 in a binary system and co-eliminated the dye and four heavy metals in a complex mixture.

3.4. Cd removal mechanism

To understand how *P. aeruginosa* Gb30 was able to resist or tolerate the presence of heavy metals in complex dye-metal contaminated mixtures, biosorption and bioaccumulation mechanisms were assessed. Quantification of Cd in pelleted bacteria and the associated supernatant after metal desorption with EDTA solution demonstrated that almost all added Cd was present in the supernatant; it was not detected in the cell pellet. Incubation of the bacterial cells in the presence of EDTA, a metal chelating agent, resulted in desorption of Cd from the cell walls and release into the supernatant. Clearly, the Cd accumulated onto the bacterial cell surface suggesting that Cb30 used biosorption to avoid heavy metal transport across the cell membrane, instead of accumulating Cd inside the cell. Giovanella et al. (2017) obtained similar results, confirming that large amounts of Cd, Ni and Pb accumulated on the surface of *Pseudomonas* sp. B50D cell walls.

Cd biosorption onto bacterial biomass was previously described by Huang and Liu (2013) and Ziagova et al. (2007). Cd binding occurs by a combined or single biosorption process, including physical adsorption, ion exchange, complex formation and precipitation (Ayangbenro and Babalola, 2017; Hansda et al., 2016). In Gram-negative bacteria, cell membrane phosphate groups in phospholipids and lipo-polysaccharides were the primary sites for metal binding (Beveridge and Murray 1980). Moreover, *Pseudomonas* species are well known for their abilities to synthesize extracellular polymers with important roles in metal chelation (Gupta and Diwan, 2017). Giovanella et al., (2017) showed that *Pseudomonas* sp. B50D used reduction, biosorption, siderophore production and biofilm formation in the bio-removal of metals.

3.5. Morphological characterization

3.5.1. FTIR

FTIR scanning of *Pseudomonas aeruginosa* biomass revealed the presence of all the typical peaks corresponding to the major cell components (lipids, proteins, nucleic acids and carbohydrates) with functional groups including carboxyl, hydroxyl, aldehydes, ketones amide and phosphates which may be involved in heavy metal uptake (Fig.5). In the 3800-2800 cm^{-1} region several bands were prominent: the band at 3272 cm^{-1} corresponded to stretching vibration of bonded- and non-bonded hydroxyl groups and water. Peaks at 2924 and 2848 cm^{-1} indicated the presence of both symmetrical and asymmetrical C-H stretching, corresponding to aliphatic methylene groups. The sharp peak at 1641 cm^{-1} is attributed to stretching vibration by C=C, C=O and COO- groups of cyclic alkenes, ketones, aldehydes and carboxylic acids. The peak at 1540 cm^{-1} could be explained by the presence of amide I and amide II stretching in cell proteins, whereas the peak at 1457 cm^{-1} was due to CH_2 binding of lipids. The peak at 1394 cm^{-1} is due to vibration of C-O groups in carboxylate ions. Nucleic acid and phospholipids cause asymmetric stretching of PO_2^- groups, producing a peak at 1235 cm^{-1}. Vibration of C-O-C, C-O, C-O-H, C-O-P groups in esters, phosphodiesters and polysaccharides results in a peak at 1077 cm^{-1}.

FTIR analysis of *P. aeruginosa* cell biomass showed differences between Cd-treated and control cells. There was a small decrease in the band at 1077 cm^{-1} and new peaks appeared at 1028 cm^{-1} and 891 cm^{-1}, indicating increases in phosphodiesters and polysaccharides involved in metal binding on the cell surface . C–OH, and C–O–C groups may also be involved in Cd binding (Tarangini, 2009). These results agree with reports demonstrating extracellular polymeric substances (EPS) produced by microorganisms in complex formation with heavy metals. For example, Boggs et al. (2016) showed that cell-bound EPS of *Pseudomonas* sp. strain EPS-1W facilitated redox transformation and sorption of Pu on the cell surface.

3.5.2. SEM analysis

Pseudomonas aeruginosa Gb30 cells were rod-shaped with a smooth surface when cultivated in Cd-free medium. Cells formed agglomerates and dividing cells were present. Following exposure to 70 mg L^{-1} Cd^{2+}, little change in cell size was observed (Fig.6). Size reduction is considered a mechanism adopted by micro-organisms to cope with the environmental stress; similar findings were reported by Naik and Dubey (2011) and Zeng et al. (2009), respectively, when *P. aeruginosa* strain 4EA was exposed to 0.8 mM Pb or *P. aeruginosa* strain E_1 was cultured in medium with 3 m mol L^{-1} Cd. A significant reduction in *Pseudomonas* sp. B50D cell size when exposed to 1 m mol L^{-1} Cd was also described by Giovanella et al., (2017). Further morphological changes were also previously described, including increases in cell fimbriae (Giovanella et al., 2017) or the formation of filamentous shapes (Chakravarty and Banerjee, 2008; Mohamed Fahmy Gad El-Rab et al., 2006).

3.5.3. AFM

Surface changes on Cd-treated *P. aeruginosa* Gb30 cells were investigated using AFM microscopy in comparison with untreated cells. The length, width and height of the control cells were 1.23±0.13, 0.63±0.06 and 0.517±0.08 µm, respectively. In the presence of 70 mg L^{-1} Cd, no significant changes in cell length, width or height occurred ($P \geq 0.05$), corroborating the SEM results. To evaluate the impact of Cd on the cell surface, roughness analysis was used, as the measurement describes changes in surface topography. Consistent with the adsorption analysis results, the surface of control cells was relatively homogeneous with an R_{rms} value = 32.53±4.72 nm but on exposure to Cd became significant heterogeneity with an R_{rms} value = 65.14±12.94 nm ($P \leq 0.05$). These results supported the previous suggestion that Cd removal by strain Gb30 included surface adsorption. Although external proteins and lipopolysaccharides regulate surface changes of Gram-negative bacteria in stressful conditions, Ramya and Thatheyu (2018) reported that exposure of bacteria to heavy metals leads to changes in the surface architecture of the outer membrane as reflected by an increase in roughness.

4. Conclusion

Co-removal of dyes and heavy metals by *Pseudomonas aeruginosa* Gb30 in culture was demonstrated. The bacterial strain exhibited effectively removed Cd from culture fluids, with simultaneously detoxifying the dye RB5. The strain was highly tolerant/resistant to the presence of a heavy metals mixture, and able to remove zinc, copper and chromium ions in addition to Cd. The mechanism of Cd removal was adsorption. The performance of *P. aeruginosa* Gb30 in simultaneous removal of dyes and heavy metals makes the strain an attractive candidate for the bioremediation of multiple contaminants in wastewaters.

Acknowledgments

This work was supported by the Ministry of Higher Education and Scientific Research of Tunisia. Special thanks to the Materials Engineering Department of the National School of Engineers of Sfax for help in FTIR spectroscopy analysis and the Digital Research Center of Sfax (CRNS) for support in AFM spectroscopy.

Conflict of interest

The authors declare no conflict of interest

5. References

Aksu, Z., 2005. Application of biosorption for the removal of organic pollutants: a review. Process Biochem. 40, 997–1026. https://doi.org/10.1016/j.procbio.2004.04.008

Ali, N., Hameed, A., Ahmed, S., 2009. Physicochemical characterization and Bioremediation perspective of textile effluent, dyes and metals by indigenous Bacteria. J. Hazard. Mater. 164, 322–328. https://doi.org/10.1016/j.jhazmat.2008.08.006

Ali, N.F., El-Mohamedy, R.S.R., 2012. Microbial decolourization of textile waste water. J. Saudi Chem. Soc. 16, 117–123. https://doi.org/10.1016/j.jscs.2010.11.005

Anwar, F., Hussain, S., Ramzan, S., Hafeez, F., Arshad, M., Imran, M., Maqbool, Z., Abbas, N., 2014. Characterization of Reactive Red-120 Decolorizing Bacterial Strain *Acinetobacter junii* FA10 Capable of Simultaneous Removal of Azo Dyes and Hexavalent Chromium. Water. Air. Soil Pollut. 225. https://doi.org/10.1007/s11270-014-2017-7

Aryal, M., Liakopoulou-Kyriakides, M., 2015. Bioremoval of heavy metals by bacterial biomass. Environ. Monit. Assess. 187. https://doi.org/10.1007/s10661-014-4173-z

Ayangbenro, A., Babalola, O., 2017. A New Strategy for Heavy Metal Polluted Environments: A Review of Microbial Biosorbents. Int. J. Environ. Res. Public. Health 14, 94. https://doi.org/10.3390/ijerph14010094

Ben Mansour, H., Mosrati, R., Corroler, D., Ghedira, K., Barillier, D., Chekir, L., 2009. In vitro mutagenicity of Acid Violet 7 and its degradation products by Pseudomonas putida mt-2: Correlation with chemical structures. Environmental Toxicology and Pharmacology 27, 231–236. https://doi.org/10.1016/j.etap.2008.10.008

Bernhoft, R.A., 2013. Cadmium Toxicity and Treatment. Sci. World J. 2013, 1–7. https://doi.org/10.1155/2013/394652

Beveridge, T.J., Murray, R.G., 1980. Sites of metal deposition in the cell wall of *Bacillus subtilis*. J. Bacteriol. 141, 876–887.

Boggs, M., Jiao, Y., Dai, Z., Zavarin, M., Kersting, A., 2016. Plutonium Interactions with Pseudomonas sp. and its Extracellular Polymeric Substances. Applied and Environmental Microbiology 82, AEM.02572-16. https://doi.org/10.1128/AEM.02572-16

Chakravarty, R., Banerjee, P.C., 2008. Morphological changes in an acidophilic bacterium induced by heavy metals. Extremophiles 12, 279–284. https://doi.org/10.1007/s00792-007-0128-4

Chao, Y., Zhang, T., 2011. Optimization of fixation methods for observation of bacterial cell morphology and surface ultrastructures by atomic force microscopy. Appl. Microbiol. Biotechnol. 92, 381–392. https://doi.org/10.1007/s00253-011-3551-5

Dellai, A., Dridi, D., Lemorvan, V., Robert, J., Cherif, A., Mosrati, R., Mansour, H.B., 2013. Decolorization does not always mean detoxification: case study of a newly isolated *Pseudomonas peli* for decolorization of textile wastewater. Environ Sci Pollut Res 20, 5790–5796. https://doi.org/10.1007/s11356-013-1603-3

Durai, G., Rajasimman, M., 2011. Biological Treatment of Tannery Wastewater - A Review. J. Environ. Sci. Technol. 4, 1–17. https://doi.org/10.3923/jest.2011.1.17

Feki-Tounsi, M., Olmedo, P., Gil, F., Khlifi, R., Mhiri, M.-N., Rebai, A., Hamza-Chaffai, A., 2013. Cadmium in blood of Tunisian men and risk of bladder cancer: interactions with arsenic exposure and smoking. Environ. Sci. Pollut. Res. 20, 7204–7213. https://doi.org/10.1007/s11356-013-1716-8

Fenta, M.M., 2014. Heavy Metals Concentration in Effluents of Textile Industry, Tikur Wuha River and Milk of Cows Watering on this Water Source, Hawassa, Southern Ethiopia. Res. J. Environ. Sci. 8, 422–434. https://doi.org/10.3923/rjes.2014.422.434

Giovanella, P., Cabral, L., Costa, A.P., de Oliveira Camargo, F.A., Gianello, C., Bento, F.M., 2017. Metal resistance mechanisms in Gram-negative bacteria and their potential to remove Hg in the presence of other metals. Ecotoxicol. Environ. Saf. 140, 162–169. https://doi.org/10.1016/j.ecoenv.2017.02.010

Gui, M., Chen, Q., Ma, T., Zheng, M., Ni, J., 2017. Effects of heavy metals on aerobic denitrification by strain Pseudomonas stutzeri PCN-1. Appl. Microbiol. Biotechnol. 101, 1717–1727. https://doi.org/10.1007/s00253-016-7984-8

Gupta, P., Diwan, B., 2017. Bacterial Exopolysaccharide mediated heavy metal removal: A Review on biosynthesis, mechanism and remediation strategies. Biotechnol. Rep. 13, 58–71. https://doi.org/10.1016/j.btre.2016.12.006

Hansda, A., Kumar, V., Anshumali, 2016. A comparative review towards potential of microbial cells for heavy metal removal with emphasis on biosorption and bioaccumulation. World J. Microbiol. Biotechnol. 32. https://doi.org/10.1007/s11274-016-2117-1

Huang, G., Wang, W., Liu, G., 2015. Simultaneous chromate reduction and azo dye decolourization by Lactobacillus paracase CL1107 isolated from deep sea sediment. J. Environ. Manage. 157, 297–302. https://doi.org/10.1016/j.jenvman.2015.04.031

Huang, W., Liu, Z., 2013. Biosorption of Cd(II)/Pb(II) from aqueous solution by biosurfactant-producing bacteria: Isotherm kinetic characteristic and mechanism studies. Colloids Surf. B Biointerfaces 105, 113–119. https://doi.org/10.1016/j.colsurfb.2012.12.040

Imran, M., Shaharoona, B., Crowley, D.E., Khalid, A., Hussain, S., Arshad, M., 2015. The stability of textile azo dyes in soil and their impact on microbial phospholipid fatty acid profiles. Ecotoxicol. Environ. Saf. 120, 163–168. https://doi.org/10.1016/j.ecoenv.2015.06.004

Kolekar, Y.M., Kodam, K.M., 2012. Decolorization of textile dyes by *Alishewanella sp.* sp. KMK6. Appl Microbiol Biotechnol 95, 521–529. https://doi.org/10.1007/s00253-011-3698-0

Lacave, J.M., Bilbao, E., Gilliland, D., Mura, F., Dini, L., Cajaraville, M.P., Orbea, A., 2020. Bioaccumulation, cellular and molecular effects in adult zebrafish after exposure to cadmium sulphide nanoparticles and to ionic cadmium. Chemosphere 238, 124588. https://doi.org/10.1016/j.chemosphere.2019.124588

Louati, I., Hadrich, B., Nasri, M., Belbahri, L., Woodward, S., Mechichi, T., 2019. Modelling of Reactive Black 5 decolourization in the presence of heavy metals by the newly isolated *Pseudomonas aeruginosa* strain Gb30. Journal of Applied Microbiology 126, 1761–1771. https://doi.org/10.1111/jam.14262

Mahmood, S., Khalid, A., Arshad, M., Mahmood, T., Crowley, D.E., 2015. Detoxification of azo dyes by bacterial oxidoreductase enzymes. Crit. Rev. Biotechnol. 1–13. https://doi.org/10.3109/07388551.2015.1004518

Maqbool, Z., Hussain, S., Ahmad, T., Nadeem, H., Imran, M., Khalid, A., Abid, M., Martin-Laurent, F., 2016. Use of RSM modeling for optimizing decolorization of simulated textile wastewater by Pseudomonas aeruginosa strain ZM130 capable of simultaneous removal of reactive dyes and hexavalent chromium. Environ. Sci. Pollut. Res. 23, 11224–11239. https://doi.org/10.1007/s11356-016-6275-3

Mishra, A., Malik, A., 2014. Metal and dye removal using fungal consortium from mixed waste stream: Optimization and validation. Ecol. Eng. 69, 226–231. https://doi.org/10.1016/j.ecoleng.2014.04.007

Mohamed Fahmy Gad El-Rab, S., Abdel-Fattah Shoreit, A., Fukumori, Y., 2006. Effects of Cadmium Stress on Growth, Morphology, and Protein Expression in *Rhodobacter capsulatus* B10. Biosci. Biotechnol. Biochem. 70, 2394–2402. https://doi.org/10.1271/bbb.60122

Naik, M.M., Dubey, S.K., 2011. Lead-Enhanced Siderophore Production and Alteration in Cell Morphology in a Pb-Resistant Pseudomonas aeruginosa Strain 4EA. Curr. Microbiol. 62, 409–414. https://doi.org/10.1007/s00284-010-9722-2

Pavlaki, M.D., Araújo, M.J., Cardoso, D.N., Silva, A.R.R., Cruz, A., Mendo, S., Soares, A.M.V.M., Calado, R., Loureiro, S., 2016. Ecotoxicity and genotoxicity of cadmium in different marine trophic levels. Environ. Pollut. 215, 203–212. https://doi.org/10.1016/j.envpol.2016.05.010

Pizzaia, D., Nogueira, M.L., Mondin, M., Carvalho, M.E.A., Piotto, F.A., Rosario, M.F., Azevedo, R.A., 2019. Cadmium toxicity and its relationship with disturbances in the cytoskeleton, cell cycle and chromosome stability. Ecotoxicology. https://doi.org/10.1007/s10646-019-02096-0

Ramya, D., Thatheyus, A.J., 2018. Microscopic Investigations on the Biosorption of Heavy Metals by Bacterial Cells: A Review. Sci. Int. 6, 11–17. https://doi.org/10.17311/sciintl.2018.11.17

Rani, A., Kumar, A., Lal, A., Pant, M., 2014. Cellular mechanisms of cadmium-induced toxicity: a review. Int. J. Environ. Health Res. 24, 378–399. https://doi.org/10.1080/09603123.2013.835032

Ruta, L., Paraschivescu, C., Matache, M., Avramescu, S., Farcasanu, I.C., 2010. Removing heavy metals from synthetic effluents using “kamikaze” Saccharomyces cerevisiae cells. Appl. Microbiol. Biotechnol. 85, 763–771. https://doi.org/10.1007/s00253-009-2266-3

Sarker, B., Baten, M.A., Haque, M.E.-U., Das, A., Hossain, A., Hasan, M.Z., 2015. Heavy Metals’ Concentration in Textile and Garments Industries’ Wastewater of Bhaluka Industrial Area, Mymensingh, Bangladesh. Curr. World Environ. 10, 61–66. https://doi.org/10.12944/CWE.10.1.07

Solís, M., Solís, A., Pérez, H.I., Manjarrez, N., Flores, M., 2012. Microbial decolouration of azo dyes: A review. Process Biochem. 47, 1723–1748. https://doi.org/10.1016/j.procbio.2012.08.014

Soni, R.K., Acharya, P.B., Modi, H.A., 2014. Effect of some metals on growth of Pseudomonas aeruginosa ARSKS20 and its decolorization ability of reactive red 35. Int J Curr Microbiol Appl Sci 3, 411–419.

Tarangini, K., 2009. Biosorption of heavy metals using individual and mixed cultures of Pseudomonas aeruginosa and Bacillus subtilis. National institute of technology, rourkela.

Taştan, B.E., Ertuğrul, S., Dönmez, G., 2010. Effective bioremoval of reactive dye and heavy metals by Aspergillus versicolor. Bioresour. Technol. 101, 870–876. https://doi.org/10.1016/j.biortech.2009.08.099

Tchounwou, P.B., Yedjou, C.G., Patlolla, A.K., Sutton, D.J., 2012. Heavy Metal Toxicity and the Environment, in: Luch, A. (Ed.), Molecular, Clinical and Environmental Toxicology. Springer Basel, Basel, pp. 133–164. https://doi.org/10.1007/978-3-7643-8340-4_6

Zeng, X., Tang, J., Liu, X., Jiang, P., 2009. Isolation, identification and characterization of cadmium-resistant Pseudomonas aeruginosa strain E1. J. Cent. South Univ. Technol. 16, 416–421. https://doi.org/10.1007/s11771-009-0070-y

Ziagova, M., Dimitriadis, G., Aslanidou, D., Papaioannou, X., Litopoulou Tzannetaki, E., Liakopoulou-Kyriakides, M., 2007. Comparative study of Cd(II) and Cr(VI) biosorption on Staphylococcus xylosus and Pseudomonas sp. in single and binary mixtures. Bioresour. Technol. 98, 2859–2865. https://doi.org/10.1016/j.biortech.2006.09.043

Fig.1

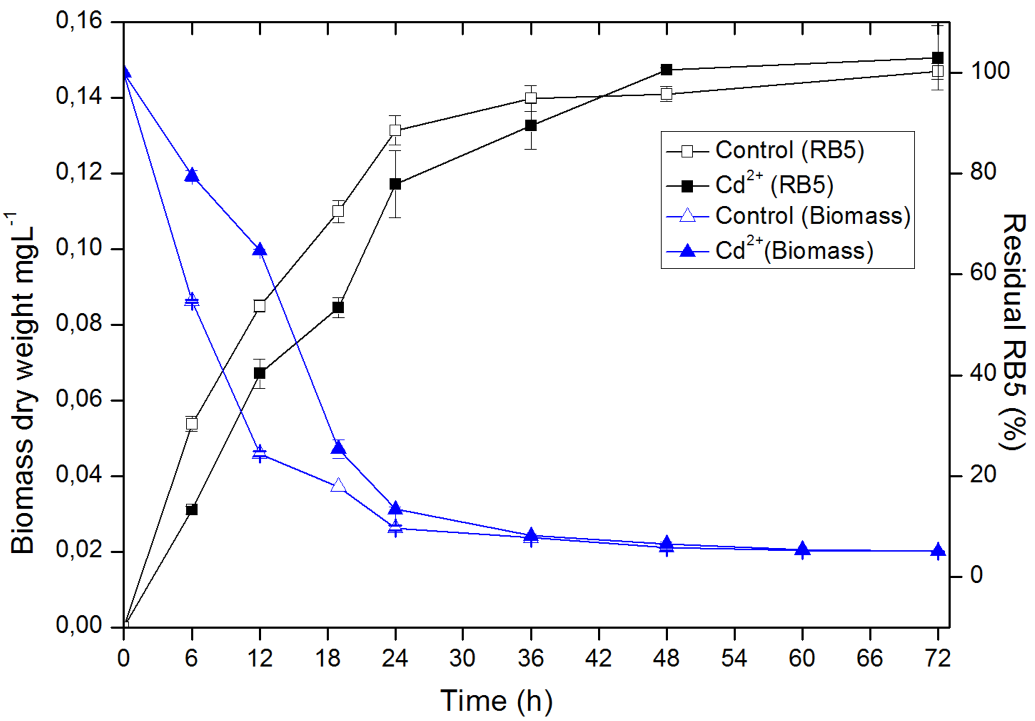

Figure 1: Bacterial dry weight (left) and decolorization kinetics of RB5 (right) in presence (■/▲) or absence (□/△) of EC50 (10h) concentrations of Cd^{2+}.

Fig.2

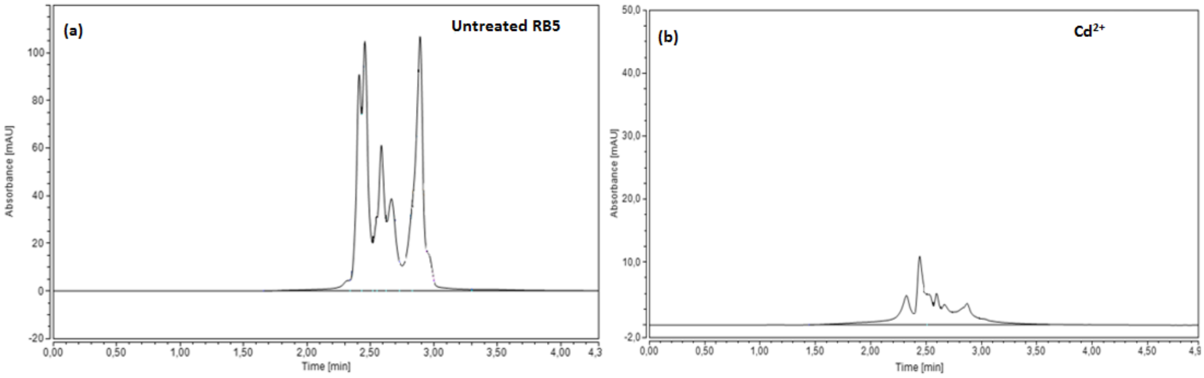

Figure 2: HPLC chromatograms of untreated RB5 (a) and its biodegradation products in presence of cadmium (b). HPLC conditions: C-18 column at room temperature with a water / methanol (60 / 40 %) flow rate of 1 mL min^{-1}.

Fig.3

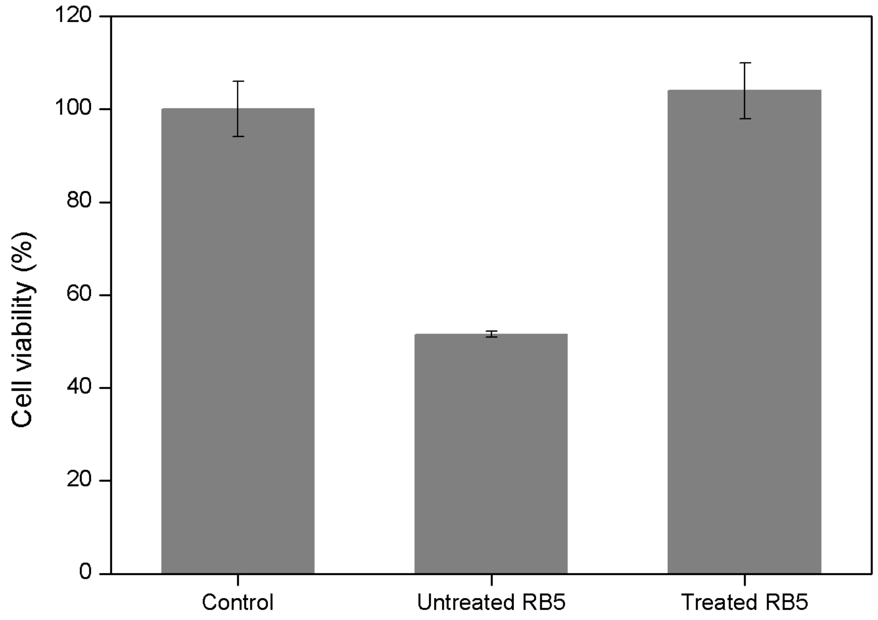

Figure 3: Cytotoxic effects of RB5 on HEK293 cells before biodegradation (Untreated RB5) and after bacterial treatment with *P. aeruginosa* strain Gb30 (Treated RB5) compared to normal cells (control).

Fig.4

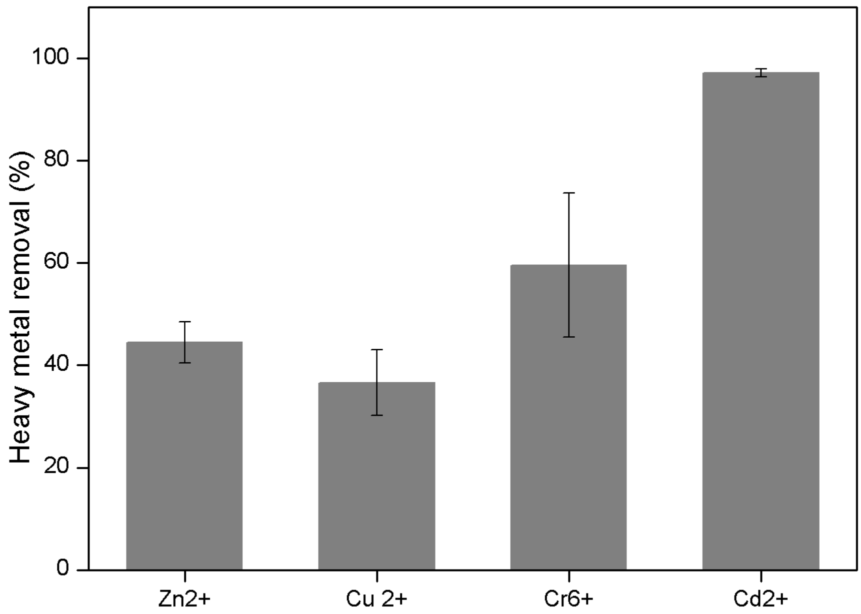

Figure 4: Removal of heavy metals from *P. aeruginosa* Gb30 cultures containing a mixture of Cr^{6+}, Cd^{2+}, Cu^{2+} and Zn^{2+} at 0.115, 0.157, 0.401 and 0.381 m mol L^{-1}, respectively, determined using atomic absorption.

Fig.5

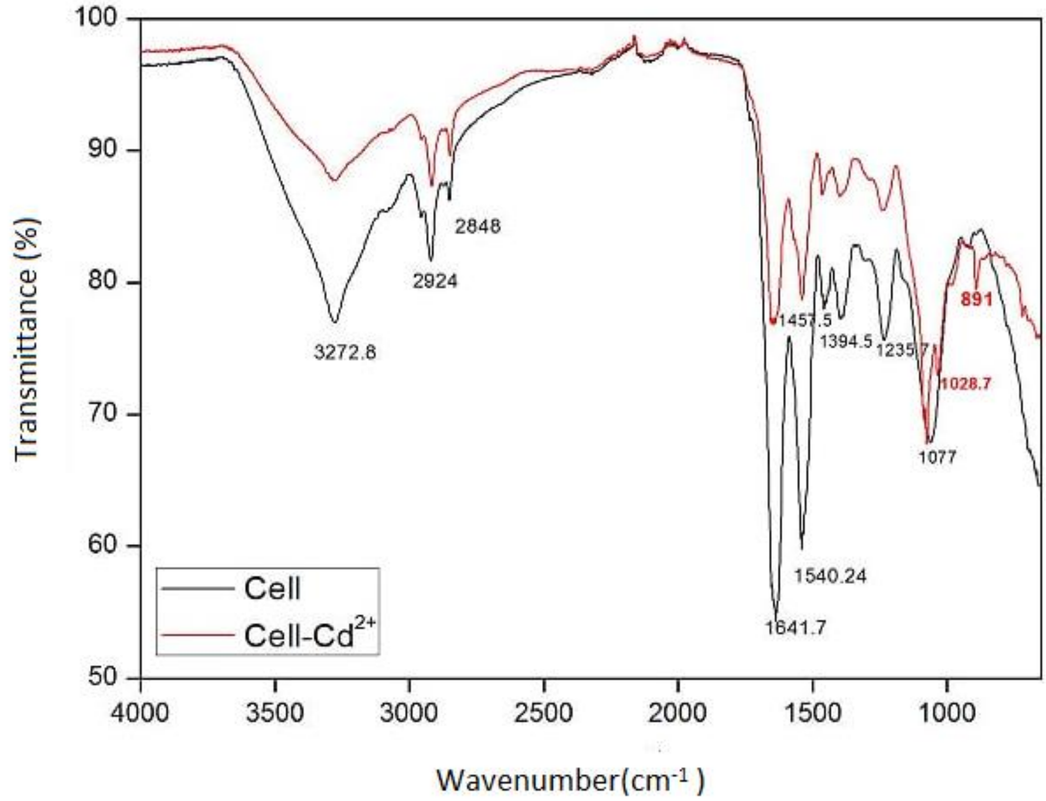

Figure 5: FTIR spectra of *Pseudomonas aeruginosa* Gb30 biomass before (Black line) and after exposure to Cd (Red line).

Fig.6

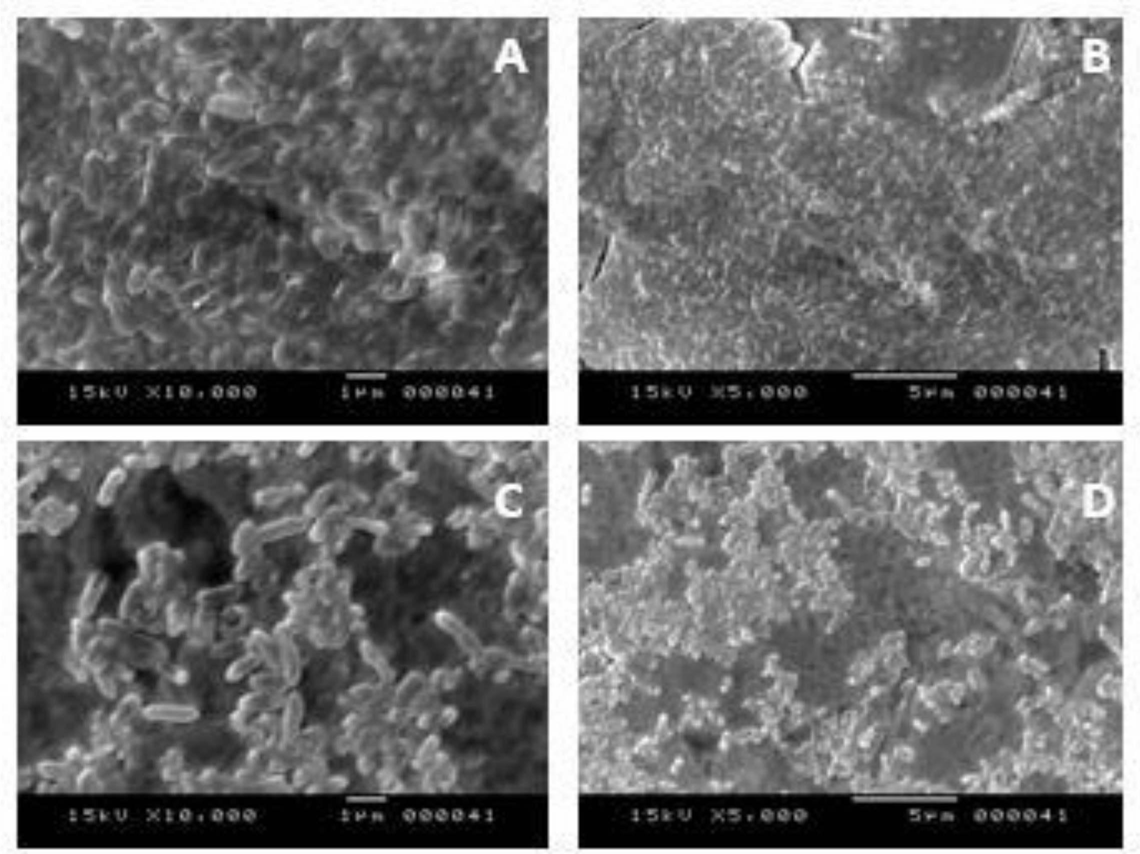

Figure 6: SEM micrographs of *Pseudomonas aeruginosa* in Cd-free medium (A, B) and Cd-containing medium (C, D).

Table 1: Kinetic constants and statistical parameters of cadmium biosorption onto biomass of *Pseudomonas aeruginosa* Gb30.

Model	k_1 (h^{-1})	k_2 (mg g^{-1} h)	q_{eq} (mg g^{-1})	R^2	R^2_{Adj}	SSE	RMSE
Pseudo-first order	0.1368	-	548.2	0.9892	0.9866	2571	25.35
Pseudo-second order	-	0.0005161	583.7	0.9774	0.9717	5407	36.77